



Title	Hierarchical classification of land use types using multiple vegetation indices to measure the effects of urbanization
Author(s)	Shishir, Sharmin; Tsuyuzaki, Shiro
Citation	Environmental monitoring and assessment, 190(6), 342 https://doi.org/10.1007/s10661-018-6714-3
Issue Date	2018-06
Doc URL	http://hdl.handle.net/2115/74518
Rights	The final publication is available at link.springer.com
Type	article (author version)
Additional Information	There are other files related to this item in HUSCAP. Check the above URL.
File Information	EMAS-D-17-03605_Revised_manuscript -.pdf



[Instructions for use](#)

1 **Hierarchical classification of land use types using multiple vegetation**
2 **indices to measure the effects of urbanization**

3 Sharmin Shishir^{a*} and Shiro Tsuyuzaki^b

4 ^aGraduate School of Environmental Science, Hokkaido University, Sapporo, 060-0810, Japan.

5 ^bGraduate School of Environmental Earth Science, Hokkaido University, Sapporo, 060-0810, Japan.

6 ORCID: 0000-0003-3010-8699

7 *Corresponding author: Sharmin Shishir (✉)

8 Graduate School of Environmental Science, Hokkaido University, N-10 W-5, North Ward, 060-

9 0810, Sapporo, Japan. tel: +81-11-706-2282, fax: +81-11-706-4954,

10 e-mail: s_shishir@eis.hokudai.ac.jp.

11 ORCID: 0000-0003-4094-7242

12 **Introduction**

13 Since the construction of new towns within natural ecosystems can cause the rapid
14 deterioration of endangered and threatened ecosystems and landscape diversities therein, it is
15 necessary to predict the effects of land use changes to promote the conservation and
16 restoration of ecosystems prior to urbanization. Fine-resolution data are desirable for
17 detecting land use changes as a result of urbanization; accordingly, the resolution of land use
18 maps should be sufficiently fine for detecting the effects of road networks and of related
19 human impacts on adjacent areas (Nigam 2000; Erener et al. 2012; Akay and Sertel 2016).

20 However, due to the lack of high-resolution data, such detailed analyses are scarce (Fonji and
21 Taff 2014; Kalyani and Govindarajulu 2015). Two satellites, namely, IKONOS and
22 WorldView-2 (WV2), recently provided high-resolution data with a resolution of less than 1
23 m (Aguilar et al. 2013). Such a resolution is likely to be suitable for analyzing land use
24 changes caused by urbanization (Nouri et al. 2014), although the effectiveness of these
25 datasets has not been examined. Therefore, the prime objective of the present study is to
26 validate the applicability of these high-resolution satellite data to the detection of land use
27 changes caused by urbanization.

28 The vegetation index (VI) was developed to detect the characteristics of vegetation
29 and land use via the combination of two or more wavelength bands related to photosynthesis,
30 i.e., the blue, green, red and near-infrared bands (Huete et al. 1999). A high VI indicates a
31 high vegetation greenness related to the high activities and low stresses of plants, and vice
32 versa (Rocha and Shaver 2009). Therefore, VIs are often applied to analyses of land use and
33 vegetation changes, e.g., to detect spatial variabilities (Matsushita et al. 2007), plant cover
34 distributions and densities (Myneni et al. 1997; Saleska et al. 2007) and temporal changes
35 (Lunetta et al. 2006). To evaluate the greenness of the ground surface, various VIs have been
36 proposed (Joshi and Chandra 2011; Barzegar et al. 2015), and they are represented by the
37 normalized difference vegetation index (NDVI), enhanced vegetation index (EVI), two-band
38 enhanced vegetation index (EVI2) and green-red vegetation index (GRVI) (Jiang et al. 2007).

39 The NDVI is widely used to detect land use-land cover (LULC) changes (Sahebjalal
40 and Dashtekian 2013; Singh et al. 2016). Additionally, measurements of the NDVI are
41 employed to broadly assess the spatiotemporal characteristics of LULC, including the
42 vegetation cover (Kinthada et al. 2014). The principle of the NDVI is derived from the
43 reflectance characteristics of photosynthesis, i.e., through an examination of the vegetation
44 greenness by using red band signals absorbed by plants and near-infrared band signals

45 reflected by plants (Rouse et al. 1974). The weakness of this index lies in the fact that
46 atmospheric and/or ground surface conditions, such as clouds and soils, often distort its
47 accuracy (Kushida et al. 2015; Miura et al. 2001). Three indices, namely, the EVI, EVI2 and
48 GRVI, were developed to reduce these obstacles, and they are popularly employed in
49 addition to the NDVI (Phompila et al. 2015). The EVI enhances the greenness signal of the
50 ground surface, which includes forest canopy structures, by using the blue band (Huete et al.
51 2002) and therefore reduces soil and atmospheric interference (Holben and Justice 1981). The
52 EVI2 was modified from the EVI by removing the blue band to improve the auto-correlative
53 defects of surface reflectance spectra between the red and blue wavelengths (Jiang et al.
54 2008), particularly when the background soil reflectance fluctuates (Kushida et al. 2015). The
55 GRVI is often applied to evaluate forest degradation and canopy tree phenology, because this
56 index is sensitive to changes in the leaf color at the canopy surface by using green
57 wavelengths (Motohka et al. 2010).

58 The effectiveness of each of the abovementioned VIs has been compared well at
59 coarse scales, e.g., at 30 m with Landsat TM5 data and at 250 m with both MOD13Q1 and
60 NOAA-AVHRR imagery (Julien et al. 2011). However, only a few studies have been
61 conducted to investigate LULC changes using VI time series (Markogianni et al. 2013). Land
62 use classification schemes using VIs at a fine scale should be validated prior to examining
63 land use changes, because the accuracies of these VIs at higher resolutions have not been
64 examined thoroughly. A new planned township, namely, Purbachal New Town, is being
65 prepared on the northeastern side of Dhaka, Bangladesh (Rahman et al. 2016a). High-
66 resolution data are available for a land use comparison between the pre- and post-
67 urbanization periods. Therefore, the effectiveness of each of the four popular vegetation
68 indices, namely, the EVI2, EVI, GRVI and NDVI, were examined at a high resolution by
69 comparing the two phases of urbanization (i.e., pre-urbanization and present-day) in the new

70 township. Each VI has both strong and weak points with regard to the classification of land
71 use types (Dibs et al. 2017). To solve this issue, a decision tree (DT) was also utilized in this
72 study. The application of DTs has been increased for image classification purposes because
73 of their accuracy and interpretation capabilities. DTs are effective for categorizing and
74 selecting each class in a classification tree (Laliberte et al. 2007), and they have performed
75 successfully with remotely sensed data for the analysis of land use changes at coarse
76 resolutions (Brown de Colstoun et al. 2003, Sesnie et al. 2008), although their accuracy was
77 not examined for fine resolutions (high-resolution satellite imagery < 30 m and very high-
78 resolution ≤ 5 m) (Fisher et al. 2017).

79 The first objective in this study was to examine the efficiencies of the VIs with regard
80 to land use classification at a fine scale, because their efficiencies may differ between coarse
81 and fine resolutions. The second objective was to characterize the VIs for each land type and
82 to develop a hierarchical classification using a DT utilizing the characteristics of the
83 examined VIs. Finally, the third objective was to characterize the land use changes induced
84 by urbanization.

85 **Materials and methods**

86 Study area

87 Purbachal New Town, Bangladesh (23°49'45.53"-23°52'30.72"N and 90°28'20.18"-
88 90°32'43.26"E) was selected as the study area (Figure 1). At a large scale, Purbachal New
89 Town is located within eastern-central Bangladesh between large floodplains (i.e., the Old
90 Brahmaputra Floodplains) and terraces and is sandwiched by two rivers, namely, the Balu
91 and Sitalakkhya Rivers, on the west and east sides. The maximum mean monthly temperature
92 is 26.3°C in August, and the minimum is 12.7°C in January (Shapla et al. 2015). The annual

93 precipitation is 2,030 mm. The dry season generally ranges from December to February, and
94 the rainy season lasts from June to September (Rahman et al. 2016b). The new town project
95 was established to reduce the overpopulation in the capital city of Dhaka, the population
96 density of which was 57,167/km² in 2011 (Khatun et al. 2015). The planned area of the new
97 town is 2,489 ha (Zaman 2016). The construction started in 1995, and it did not cease until
98 2015. Prior to urbanization, the major land use types were forest (*Shorea robusta* Gaertner f.,
99 in the Dipterocarpaceae family, locally called *Sal* forest), homestead, homestead vegetation,
100 cropland, and various others (Rahman et al. 2016a).

101 The expansion of urban areas in Bangladesh was inadequately planned and controlled
102 due to truncated laws (Hossain 2013). Per the Environmental Conservation Act of 1995 and
103 the Bangladesh Environmental Conservation Rules, 1997, the preservation of natural forests
104 and privately owned commercial forests dominated by *Shorea robusta* should take priority
105 during the land development planning of Purbachal New Town. The major forest products are
106 edible fruits, timber and medicines. These preserved forests are expected to sustain endemic
107 and/or invaluable flora and fauna, although land development activities often neglect these
108 perspectives (Zaman 2016). Although the emphasis during the pre-planning stage was the in
109 situ preservation of entire forests, the idea to maintain all of the patches of *Shorea* forest was
110 later rejected because those isolated patches had already been exposed to human activities. To
111 compensate for the loss of forested area, a green belt with a width of 15 m to be produced
112 through afforestation was planned for the full perimeter of the township area (24.2 km²) with
113 a few exceptions. There were no interferences with the natural drainage systems that had
114 maintained the pristine ecosystems in the region.

115 In total, the land use types of the study area were classified into eight categories
116 (Table 4). Of those land use types, native forests with a maximum height of 36 m dominated
117 by *Shorea robusta* have maintained the highest biodiversity, and they contain numerous

118 endangered species (Gautam et al. 2006; Mandal et al. 2013). Therefore, the accurate
119 detection of the distribution of *Shorea* forest was the priority for this land use analysis. The
120 other land use types were homestead (i.e., settlement and residential areas), homestead
121 vegetation (vegetation consisting of trees, shrubs and herbs on and around the settlement),
122 cropland, grassland, agricultural low land, bare land and water bodies. In general, therefore,
123 homestead vegetation is larger than homestead. The homestead vegetation and agricultural
124 low land types also support a high biodiversity (Hasnat and Hoque 2016). Currently, the
125 forest ecosystems in the region are decreasing rapidly due to economical demands and human
126 interferences, such as overexploitation, deforestation, excessive trash buildup and
127 encroachment (Salam et al. 1999; Hassan 2004). Among the artificial land use types,
128 cropland, the major products of which are rice, jute and vegetables (e.g., cultivars consisting
129 of gourds, beans, cabbage, cauliflower and tomatoes), was distributed broadly prior to
130 urbanization (Shapla et al. 2015).

131 IKONOS and WV2 data

132 The data were obtained from the satellite imagery of IKONOS at 04:35 (GMT) on May 1,
133 2001, and at 04:44 on February 16, 2002, prior to urbanization and from WV2 imagery at
134 04:41 on December 9, 2015 (Digital Globe - Apollo Mapping, Longmont, Colorado, USA) at
135 present stage, since IKONOS terminated data acquisition after 2014 and WV started data
136 collection in October 2009. The resolutions of the IKONOS and WV2 sensors are 0.8 m (true
137 color) and 0.5 m (natural color), respectively. All of the images were devoid of clouds.

138 These remote sensing data were integrated via ArcGIS (version 10.2). Integrated
139 analyses were conducted after checking the quality of the pre-processed data to remove noise
140 and unify the georeferences. These images were re-projected onto the Bangladesh Transverse

141 Mercator (BTM) projection to record the statistics of landscape changes, because of the
142 projected coordinate system in Bangladesh (Dewan and Yamaguchi 2009).

143 Evaluation of the vegetation indices and hierarchical classification

144 The categories of land use types were matched with the land use map published by the
145 Ministry of Housing and Public Works of Bangladesh (Anonymous 2013) with a few
146 modifications adjusted to recently developed land use patterns. The modification was made
147 by establishing three land use types, cropland, grassland and bare land, all of which were
148 cultivable land in the original map (Anonymous 2013). Because the map was manufactured
149 based on various datasets consisting of topographical, geographical and historical data at a
150 fine scale, this map was utilized as a reference during the evaluation of land use
151 classifications.

152 A total of eleven VIs was investigated to confirm the accuracy of land use change
153 detection by using error matrix prior to the construction of DT. These eleven VIs were NDVI,
154 EVI2, EVI, GRVI, atmospherically resistant vegetation index (ARVI), green difference
155 vegetation index (GDVI), green normalized difference vegetation index (GNDVI), difference
156 vegetation index (DVI), normalized green (NG), ratio vegetation index (RVI) and enhanced
157 normalized difference vegetation index (ENDVI). The four examined VIs showed higher
158 than 65% overall accuracy, while the other VIs showed less than 50%. Therefore, the four
159 VIs, NDVI, EVI2, EVI, and GRVI were used for the further analysis.

160 The four examined vegetation indices were as follows:

$$161 \quad \text{NDVI} = (\text{NIR} - \text{red}) / (\text{NIR} + \text{red}) \quad (1)$$

$$162 \quad \text{GRVI} = (\text{green} - \text{red}) / (\text{green} + \text{red}) \quad (2)$$

$$163 \quad \text{EVI} = G \times (\text{NIR} - \text{red}) / (\text{NIR} + C_1 \times \text{red} - C_2 \times \text{blue} + L) \quad (3)$$

164
$$\text{EVI2} = 2.5 \times (\text{NIR} - \text{red}) / (\text{NIR} + 2.4 \times \text{red} + 1.0), \quad (4)$$

165 where near-infrared (NIR), red, green and blue represent (partially) atmospherically corrected
 166 surface reflectances, L denotes the canopy background adjustment used to address the
 167 nonlinear, differential transmittance of NIR and red wavelength radiances through a canopy,
 168 and C_1 and C_2 are the coefficients of the aerosol resistance term that uses the blue band to
 169 calibrate the aerosol influences in the red wavelength. The blue wavelength ranges from 445
 170 nm to 516 nm on IKONOS and from 450 nm to 510 nm on WV2, the green wavelength
 171 ranges from 506 nm to 595 nm on IKONOS and from 510 nm to 580 nm on WV2, the red
 172 wavelength ranges from 632 nm to 698 nm on IKONOS and from 630 nm to 690 nm on
 173 WV2, and the NIR wavelength lies between 757 nm and 863 nm on IKONOS and between
 174 765 nm and 901 nm on WV2. Therefore, the data collected by WV2 were comparable to the
 175 data acquired using the IKONOS sensor (Table 1).

176 **Table 1** The four wavelength bands on IKONOS and WV2 images

Band	Wavelength (nm)		
		IKONOS	WV2
Blue	min	445	450
	max	516	510
Green	min	506	510
	max	595	580
Red	min	632	630
	max	698	690
Near-infrared (NIR)	min	757	765
	max	863	901

177
 178 The NDVI refers to two spectral bands of the photosynthetic output, i.e., the red and
 179 near-infrared bands (Huete et al. 1997). The NDVI ranges from -1 to +1 and increases with
 180 an increase in the vegetation greenness. However, the NDVI is skewed by background

181 reflectances and atmospheric interference (Karnieli et al. 2013). In addition, the NDVI is
182 saturated in regions with a high biomass (Miura et al. 2001). To reduce these disadvantages
183 of the NDVI, multiple VIs modified from the NDVI have been developed (Phompila et al.
184 2015).

185 The GRVI uses green and red bands to assess deforestation, forest degradation and
186 canopy tree phenology (Motohka et al. 2010; Tucker 1979). The GRVI often focuses on
187 seasonal fluctuations in the greenness by evaluating the colors of leaves at the canopy surface
188 using the green band (Nagai et al. 2012).

189 The EVI was modified from the NDVI by adopting numerous coefficients within the
190 EVI algorithm (Equation 3): $L = 1$, $C_1 = 6$, $C_2 = 7.5$, and gain factor (G) = 2.5 (Rouse et al.
191 1974; Huete et al. 1994). These parameters are used to improve the sensitivity to high
192 biomass regions and the vegetation monitoring capability of the EVI by dissociating the
193 canopy background signal and diminishing atmospheric influences (Huete et al. 1999).

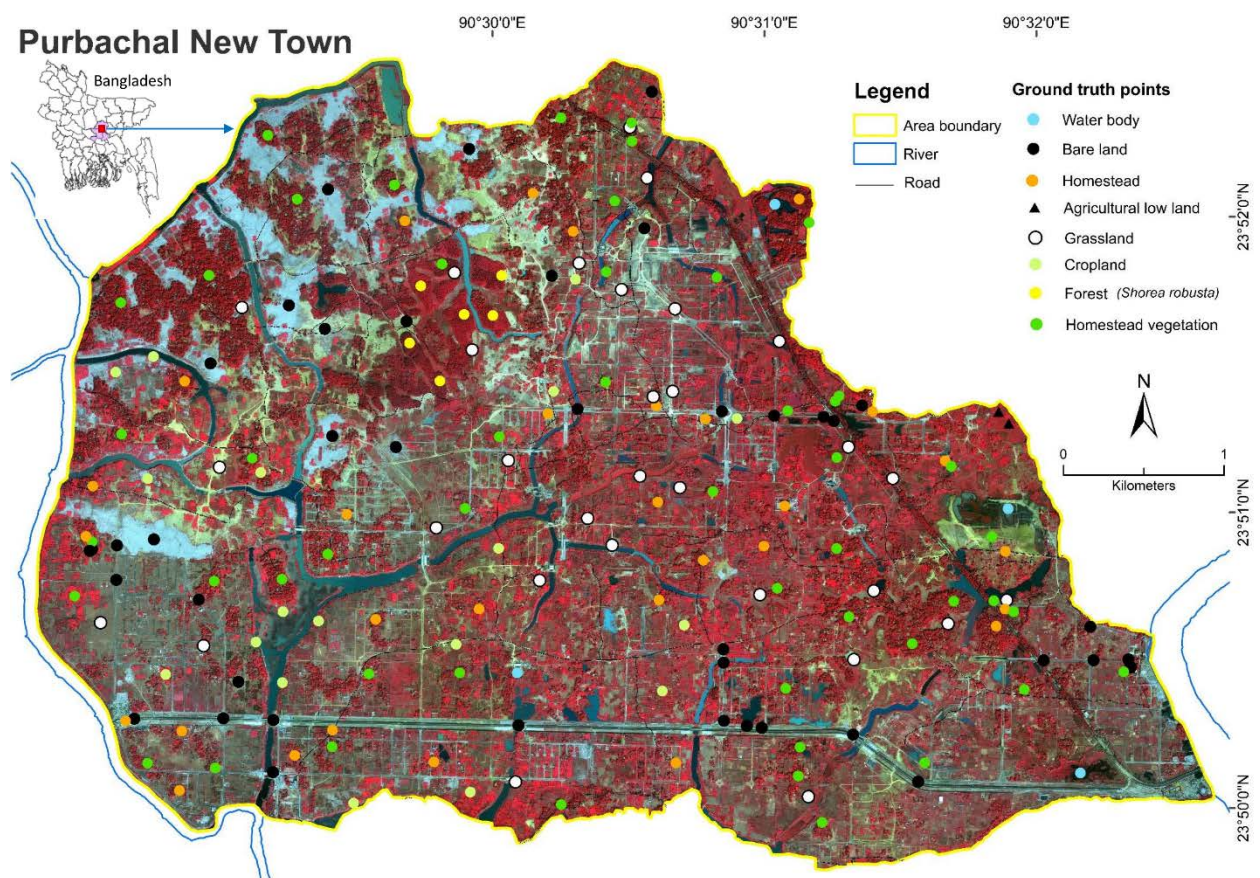
194 Although the EVI2 measures the vegetation greenness without a blue band (Equation
195 4), it resembles the 3-band EVI when the data quality is high and atmospheric effects are
196 insignificant (Jiang et al. 2008).

197 A DT classifier was applied to identify the land use types using the four examined VIs.
198 The DT was implemented depending on multiple levels of decisions based on the properties
199 of the input datasets (Mountrakis et al. 2011).

200 Accuracy assessment of the land use classification

201 Validating the land use classification is a prerequisite for confirming temporal land use
202 changes (Foody 2002). Ground truth data of stratified land use classes at 182 locations
203 marked with GPS were used for the validation (Figure 1). The ground truth points were
204 selected by using a land use map (Anonymous 2013). These locations and their adjacent areas

205 were recorded more than once to inspect the eight land use types. Based on the measurements,
 206 the land use types on the maps were repeatedly reclassified to minimize classification errors.
 207 The accuracies of the land use classification schemes using the four VIs and of the
 208 hierarchical classification using the DT classifier were tested using an error matrix
 209 represented by an overall accuracy and a κ coefficient at each ground truth point. The ESRI
 210 ArcMap (version 10.2) software was used for the data processing, including the statistical
 211 analysis.



212
 213 **Fig. 1** Image of Purbachal New Town in 2015 from the WV2 satellite. Two rivers, namely, the Balu
 214 and Sitalakhya Rivers, are distributed along the west and east sides of the township, respectively. The
 215 inset map at the top left shows Purbachal New Town in the country of Bangladesh. The 182 ground
 216 truth locations recorded via GPS in Purbachal New Town are shown on the WV2 natural color image
 217 using different colored circles for different land use types. The land use types were verified to assess
 218 the accuracy of the land use classification via satellite imagery and reference vegetation maps

219 Relationships between land use types and VIs

220 One-way analysis of variance (ANOVA) was used to investigate the significant differences in
221 the VI values among the land use types. When the ANOVA was significant, Tukey post hoc
222 multiple comparison tests were applied to determine the significant differences in the VIs
223 among the land use types confirmed using ground truth data (Zar 1999).

224 **Results**

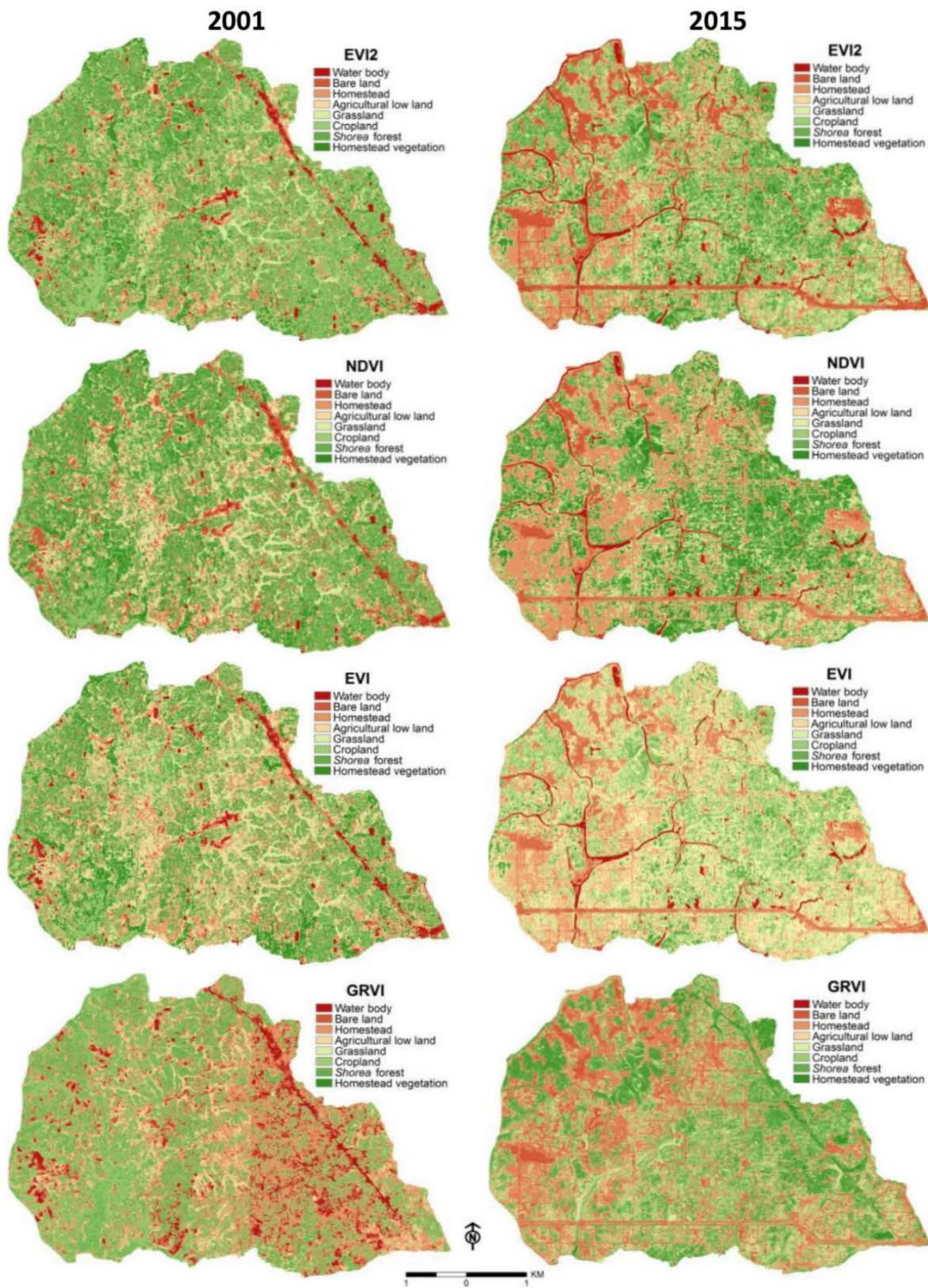
225 Surface reflectances in the VIs

226 The spatial patterns of the surface greenness in 2001 and 2015 were different among the VIs
227 (Figure 2). The GRVI effectively diagnosed the distributions of homestead vegetation and
228 *Shorea* forest but often failed to discern cropland. The EVI detected the grassland distribution
229 most correctly but could not clearly detect the *Shorea* forests. The NDVI differentiated water
230 bodies and bare land but did not delineate the *Shorea* forest and homestead vegetation land
231 use types, showing that the NDVI is not appropriate for classifying regions with dense green
232 vegetation. The EVI2 distinguished vegetated land use types from non-vegetated land use
233 types and clearly identified the homestead distribution.

234 The lowest NDVI value of -0.05 was obtained for water bodies due to the lack of
235 vegetation (Figure 3). Homestead was detected within a few small patches with a low NDVI
236 of 0.31 in 2001 and 0.21 in 2015, confirming that a fine-scale classification is required to
237 detect these land use types. Homestead vegetation (i.e., vegetation enclosing homesteads)
238 showed an NDVI of 0.91 in 2001 and 0.82 in 2015. Croplands had higher a NDVI than
239 grassland of 0.67 in 2001 and 0.59 in 2015.

240 The lowest EVI values were shown for water bodies, while the second-lowest values
241 were displayed over bare land (Table 2). The EVI did not separate these two land use types

242 clearly. The EVI of grassland was an average of 0.37, which is intermediate between the EVI
 243 values for bare land and forests. EVI values between 0.37 and 0.48 were associated with
 244 cropland and occasionally grassland, while EVI values ranging from 0.48 to 0.57 represented
 245 dense and/or deeply green vegetation.

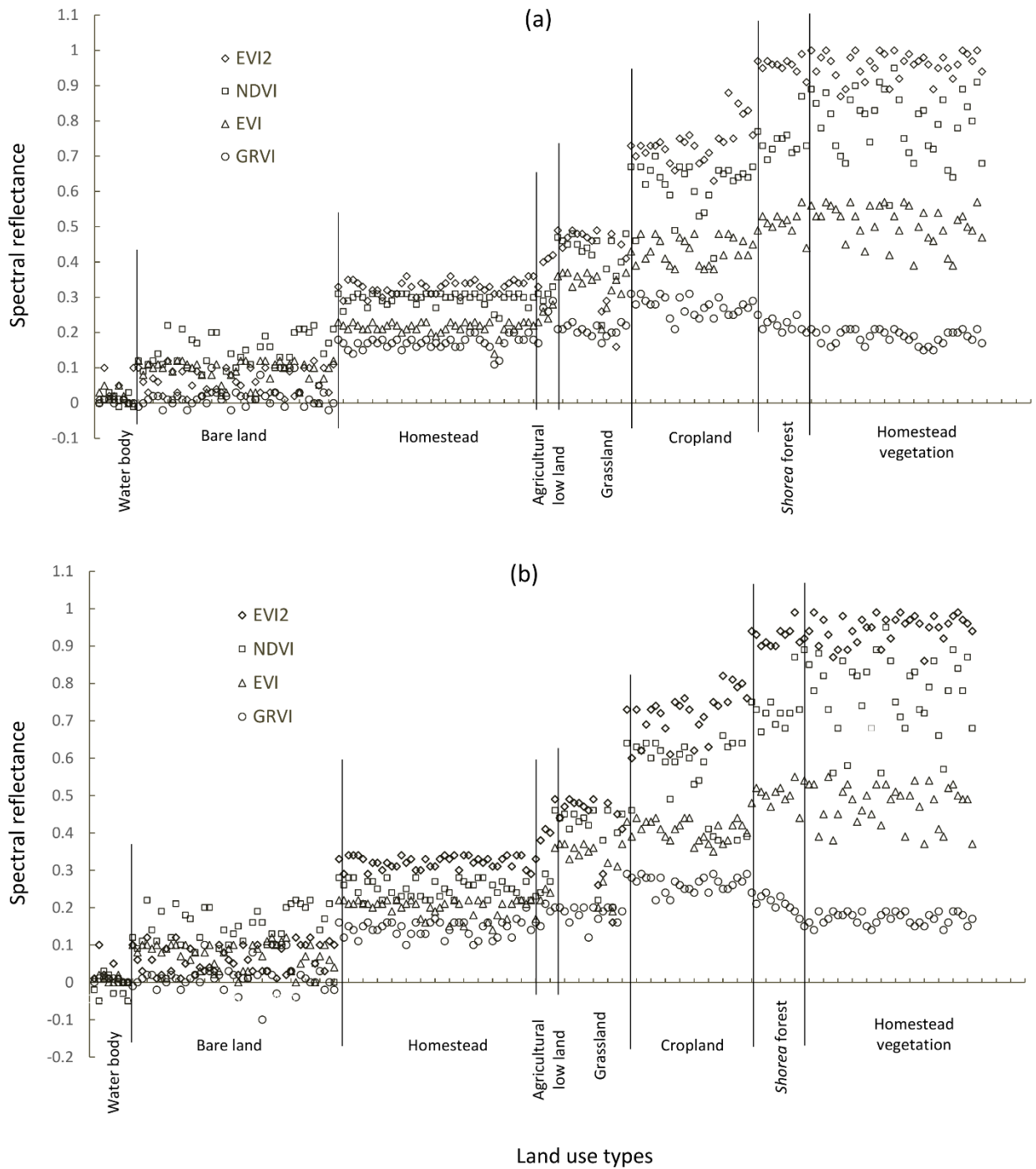


246

247 **Fig. 2** Surface greenness distributions evaluated using the four VIs based on multi-temporal
248 information from the IKONOS and WV2 images in 2001 (left side) and 2015 (right side), respectively

249 The highest EVI2 value, i.e., 1, represented dense vegetation, including homestead vegetation.
250 The EVI2 value for *Shorea* forest was 0.97, which was the highest of the examined VIs (0.77
251 with the NDVI, 0.53 with the EVI and 0.25 with the GRVI). The EVI2 value for grassland
252 ranged from 0.10 to 0.49, which is higher than those obtained with the EVI, NDVI and GRVI.
253 The EVI2 sometimes misclassified cropland as grassland, probably because of double
254 cropping. An EVI2 value lower than 0.10 indicated poorly vegetated land use types, such as
255 bare land and sparse grassland. The GRVI demonstrated an appropriate detection of densely
256 vegetated land use types, mostly due to the discrimination of *Shorea* forest and homestead
257 vegetation. However, the GRVI did not effectively discriminate among water bodies, bare
258 land and homestead (Figure 2). Non-vegetated land, i.e., water bodies and bare land, showed
259 GRVI values of less than 0.18. Bare land and water bodies showed the lowest GRVI values
260 of -0.04 and 0.01, respectively, while water bodies showed the lowest VI values overall.
261 These results indicate that the GRVI performed better while distinguishing dense vegetation
262 than other land use types characterized by sparse greenness.

263 In total, the NDVI had higher values than the EVI and GRVI, particularly when the
264 reflectance was high (Figure 3). The GRVI occasionally showed negative values over bare
265 land when it should have been higher than 0, which was probably due to soil interference. All
266 of the VIs showed a clear gap between non-vegetated and vegetated land use types. However,
267 in areas with a high vegetation, the VIs exhibited different responses to greenness.



268

269 **Fig. 3** Spectral reflectances in the VIs extracted from 182 ground truth points for eight land use
 270 classes. The y-axis indicates the spectral reflectances among the four VIs, while the x-axis represents
 271 the eight land use types

272 Validation of the VIs

273 The accuracies of the land type classification schemes were different among the VIs (Table 3).

274 Each of the four VIs showed different values among the land use types (ANOVA, $p <$
275 0.0001) (Table 2). All of the VIs showed stable values over homesteads. The EVI2 and NDVI
276 responses to grassland and cropland fluctuated, and the EVI fluctuated largely over *Shorea*
277 forest and homestead vegetation. Although the GRVI responses to *Shorea* forest and
278 homestead vegetation were stable, the GRVI responses were lower than the responses of the
279 other VIs.

280 The EVI2 exhibited different pairs of land use types except for grassland-agricultural
281 low land, agricultural low land-homestead and bare land-water body (Tukey test, $p < 0.05$).
282 The NDVI exhibited different pairs of land use types except for homestead vegetation-*Shorea*
283 forest, agricultural low land-homestead and grassland-agricultural low land. The homestead
284 vegetation-*Shorea* forest and agricultural low land-homestead pairs were not significantly
285 different in the EVI, although the rest of the pairs were different. The GRVI was capable of
286 distinguishing between homestead vegetation and *Shorea* forest, but the other three VIs could
287 not differentiate these two land use types. The GRVI did not reveal significant differences in
288 the comparisons between the other land use types ($p < 0.05$). The GRVI was most effective at
289 differentiating the *Shorea* forest-homestead vegetation pair; meanwhile, the EVI2 and NDVI
290 effectively detected homestead, bare land and water bodies, and the EVI effectively detected
291 the distributions of agricultural low land, grassland and cropland.

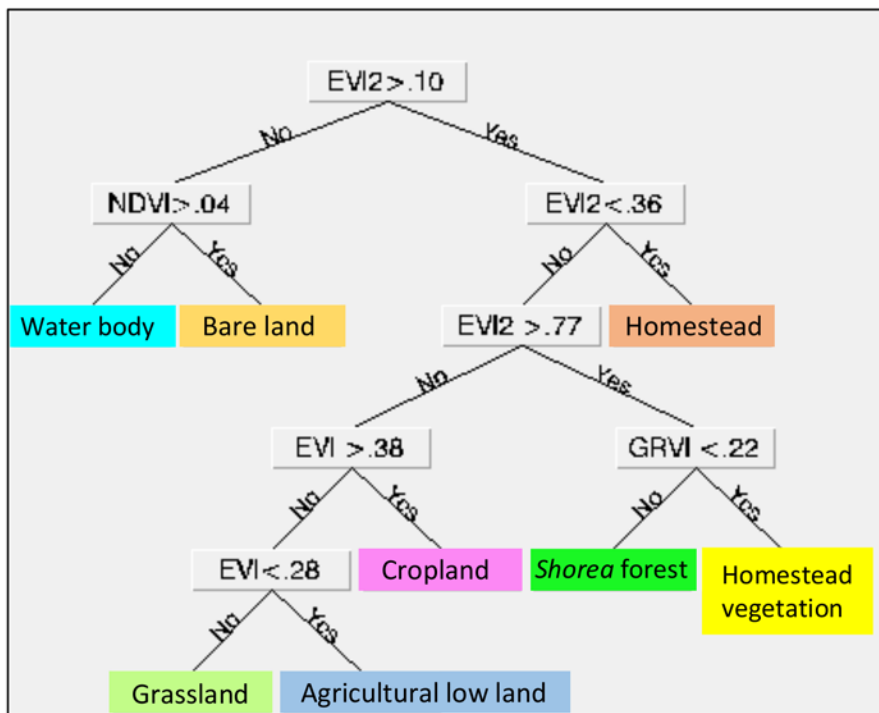
292 **Table 2** Mean and standard error (SE) of each VI for the eight land use types. All of the VIs obtained in 2001 and 2015 among the land use types
 293 are significantly different (one-way ANOVA, $p < 0.0001$). Identical letters indicate that the VIs are not significantly different between those land
 294 use types (Tukey test, $p < 0.05$)
 295

		Water body	Bare land	Homestead	Agricultural low land	Grassland	Cropland	Forest (<i>Shorea robusta</i>)	Homestead vegetation
2001	EVI2	0.04 ±0.02 a	0.06 ±0.01 a	0.32 ±0.00 b	0.42 ±0.01 c	0.42 ±0.03 c	0.74 ±0.01 d	0.96 ±0.00 e	0.96 ±0.01 e
	NDVI	0.01 ±0.01 a	0.14 ±0.01 b	0.30 ±0.00 c	0.31 ±0.01 cd	0.42 ±0.02 d	0.62 ±0.01 e	0.73 ±0.01 f	0.79 ±0.02 f
	EVI	0.02 ±0.01 a	0.09 ±0.01 b	0.22 ±0.00 c	0.26 ±0.01 c	0.34 ±0.01 d	0.43 ±0.01 e	0.51 ±0.01 f	0.51 ±0.01 f
	GRVI	0.01 ±0.00 a	0.01 ±0.01 a	0.17 ±0.00 b	0.27 ±0.01 cef	0.21 ±0.00 dfg	0.27 ±0.01 e	0.23 ±0.01 f	0.19 ±0.00 g
2015	EVI2	0.03 ±0.01 a	0.06 ±0.01 a	0.32 ±0.00 b	0.40 ±0.01 bc	0.42 ±0.03 c	0.72 ±0.01 d	0.92 ±0.01 e	0.95 ±0.01 e
	NDVI	-0.02 ±0.01 a	0.14 ±0.01 b	0.25 ±0.00 c	0.27 ±0.02 cd	0.41 ±0.02 d	0.56 ±0.02 e	0.71 ±0.01 f	0.77 ±0.02 f
	EVI	0.01 ±0.00 a	0.08 ±0.01 b	0.2 ±0.00 c	0.24 ±0.01 c	0.33 ±0.02 d	0.41 ±0.01 e	0.50 ±0.01 f	0.48 ±0.01 f
	GRVI	0.01 ±0.00 a	0.01 ±0.01 a	0.14 ±0.00 b	0.18 ±0.02 bcdf	0.18 ±0.01 ce	0.26 ±0.00 f	0.22 ±0.01 d	0.17 ±0.00 e

296 Hierarchical classification of land use types

297 A hierarchical land use classification was developed using a DT classifier with the four VIs

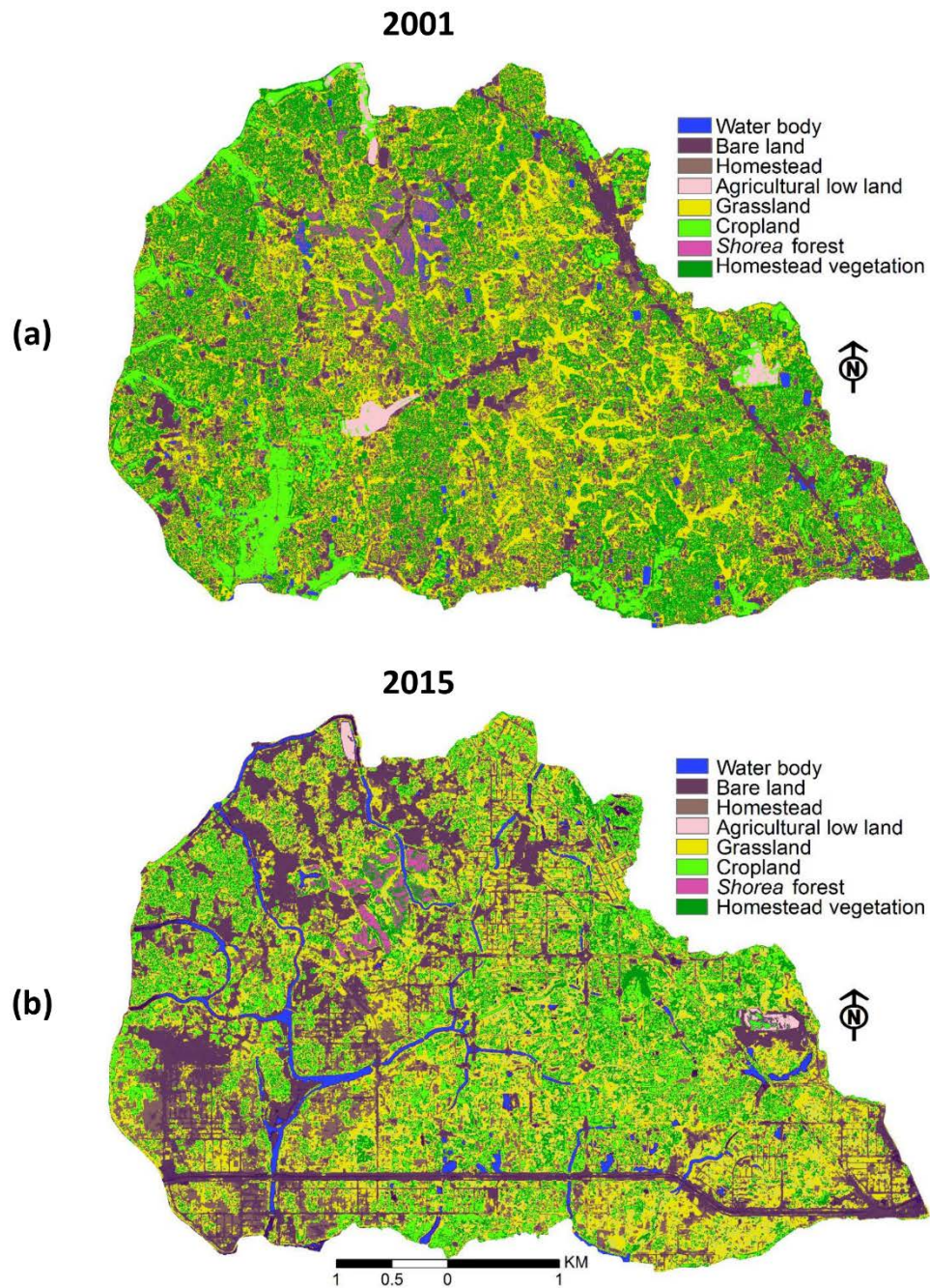
298 (Figure 4).



299

300 **Fig. 4** A DT constructed using the hierarchical classification of land use types. Numerals with inequality
301 signs indicate the VI values that represent the thresholds of the classifiers

302 The DT begins with the EVI2, which then separates the land use types into vegetated and non-
303 vegetated land use types. The NDVI then separates the non-vegetated land uses into water bodies
304 and bare land. Meanwhile, among the vegetated land use types, the EVI2 extracts the homestead
305 distribution and the EVI detects agricultural low land, grassland and cropland. Among the four
306 VIs, homestead vegetation and *Shorea* forest were separated only through the GRVI.



307

308 **Fig. 5** Land use maps produced through a hierarchical classification using the DT approach. These maps
 309 show the temporal changes in the land use-land cover throughout Purbachal New Town from 2001 to
 310 2015. a) Land use patterns detected using the IKONOS sensor in 2001. The land use patterns were
 311 verified using a pre-project land use map (Anonymous 2013). b) Land use patterns in 2015 were detected
 312 using WV2 multi-spectral imagery. The land use types are represented by their respective colors

313

Table 3 Classification accuracies examined using an error matrix of κ coefficients

Classification	2001		2015	
	Overall accuracy (%)	κ coefficient	Overall accuracy (%)	κ coefficient
EVI2	90.1	0.88	91.2	0.89
NDVI	88.5	0.86	89.6	0.87
EVI	66.5	0.60	67.6	0.61
GRVI	74.2	0.69	77.5	0.73
DT	96.1	0.95	97.8	0.97

314

The DT approach showed the highest accuracy (with an accuracy greater than 95% and a

315

κ of greater than 0.95, see Table 3) during the land use classification, indicating that the DT

316

constructed using the four VIs was the most effective at predicting the land use types (Figure 5).

317

The second-highest accuracy and κ values (91.2% and 0.89, respectively) were exhibited by the

318

EVI2 measurements from 2015, indicating that the DT effectively improved the land use

319

classification scheme.

320

LULC changes

321

Based on the land use changes from 2001 to 2015 (Figure 5), the characteristics of the land use

322

changes were examined (Table 4). Road networks and their adjacent areas were clearly observed.

323

Homestead vegetation, grassland, cropland and homestead were the dominant land use types

324

prior to urbanization, but more than three-quarters of the area of each land use type was lost

325

thereafter. Approximately one-half of the area of *Shorea* forest was lost subsequent to

326

urbanization. Since the distribution of bare land increased greatly, the reduction in the area of

327

each land use type can be derived according to an increase in bare land originating from road

328

construction and other related construction projects, and the water body area was also increased

329

due to the excavation of artificial lakes and canals. Grasses colonized in the filed up agricultural

330

low land and consequently, the grassland increased. Since most of the water bodies were small

331 and/or narrow, those changes were detectable only at a high resolution.

332 **Table 4** Changes in the eight land use types from 2001 to 2015 based on satellite imagery

Land use types	2001		2015	
	Area (km ²)	(%)	Area (km ²)	(%)
Water body	0.59	2.37	2.12	8.52
Bare land	0.14	0.56	16.97	68.17
Homestead	3.02	12.13	0.86	3.46
Agricultural low land	0.67	2.69	0.04	0.16
Grassland	1.03	4.14	1.06	4.26
Cropland	6.26	25.15	0.59	2.37
Forest (<i>Shorea robusta</i>)	0.77	3.09	0.42	1.69
Homestead vegetation	12.41	49.86	2.83	11.37

333 **Discussion**

334 Effectiveness of the VIs and the DT approach

335 A comparison among the DT and VIs indicates that all four of the examined VIs showed specific
336 advantages and disadvantages with regard to the land use classification at a fine resolution. The
337 reflectances of the blue and green wavelengths can characterize the spatiotemporal fluctuation
338 patterns of VIs (Huete 1988). The EVI2 differentiated between vegetated and non-vegetated land
339 use types without using the blue band. Only the GRVI classified dense vegetation, i.e.,
340 homestead vegetation and *Shorea* forests, probably because the GRVI is sensitive to the canopy
341 surfaces of forests (Nagai et al. 2012). Therefore, the GRVI constituted a prerequisite for the
342 classification of deeply green areas, i.e., forests, although the overall accuracy of the associated
343 classification was low.

344 The EVI2 showed the highest accuracy among the examined VIs at a fine resolution
345 (Kushida et al. 2015). However, the EVI2 did not effectively differentiate between homestead
346 vegetation and *Shorea* forest. The EVI2 maintains a high sensitivity and linearity to high
347 phytomass densities (Rocha and Shaver 2009). However, there are many difficulties when using
348 the EVI2 to conduct a land use classification in tropical/sub-tropical regions such as Bangladesh,
349 because persistent evergreen forests show high reflectances both in and out of season (Cristiano
350 et al. 2014). The accuracy of the NDVI land classification was slightly lower than that of the
351 EVI2 results. The NDVI is skewed by the background reflectance, including those of bright soils
352 and non-photosynthetic plant organs (i.e., trash and tree trunks) (Van Leeuwen and Huete 1996).
353 Because the examined data did not contain a substantial amount of clouds, the EVI2 and NDVI
354 seemed to synchronize their fluctuations.

355 The EVI effectively classified the grassland, cropland and agricultural low land types, but
356 it did not distinguish the other land use types, suggesting that the blue band used only by the EVI
357 influenced the resulting land use classification. However, the EVI is distorted by the soil
358 adjustment factor L in Equation (3), making it more sensitive to topographic conditions
359 (Wardlow et al. 2007). Therefore, the EVI did not seem to function well.

360 The DT using the four VIs largely improved the accuracy of the land use classification.
361 The accuracy of the DT was slightly different between the two surveyed years (96.1% in 2001
362 and 97.8% in 2015, see Table 3). One cause of this difference was probably derived from
363 differences in the quality of the data, i.e., with regard to the resolution, photographing conditions
364 and sensors, from IKONOS in 2001 and from WV2 in 2015.

365 Temporal land use changes caused by urbanization

366 This research used highly resolved, multi-temporal satellite data to develop a methodology for

367 assessing land use changes. The results of the VIs vary between fine and coarse resolution. The
368 fine-scale land use classification scheme clearly detected fine-scale land use patches generated
369 by the development of road networks subsequent to urbanization that cannot be detected during
370 coarse-scale analysis. Accordingly, land use classification schemes are often dependent upon the
371 resolution (O'Connell et al. 2013). Since roadways are a few tens of meters wide, high-resolution
372 data are required for the classification of urban landscapes. Fine-scale data can delineate land
373 cover classes more accurately, because such data can identify small and/or linear patches while
374 retaining their shapes (Boyle et al. 2014). Ongoing urbanization has been followed by drastic
375 changes in the land use types, biodiversity and fragile ecosystems of urbanized areas (Merlotto et
376 al. 2012; Zhou and Zhao 2013; Pigeon et al. 2006). The urbanization of Purbachal New Town
377 was characterized by a substantial loss of homestead vegetation and cultivable land. Furthermore,
378 approximately one-half of native *Shorea* forests were lost, even though the master plan of
379 urbanization considered their conservation (Hasnat and Hoque 2016). Land use changes
380 associated with deforestation have not been detected well. The endangered *Shorea* forests are
381 likely to be restored and conserved through the identification of small and isolated patches using
382 the fine-scale analysis. The species distribution modeling should be executed for the restoration
383 of the threatened ecosystems using the identified distinct small patches. Also, land
384 transformation model would be implemented using fine-scale data to show the process of land
385 use changes (Pijanowski et al. 2002). These approaches are the pronounced concern for the
386 planners to protect and preserve the endangered ecosystems from being extinction.

387 Imagery acquired by two or more satellites is often used to examine temporal land use
388 changes depending on the data availability. This study used two sets of satellite imagery, namely,
389 from the IKONOS and WV2 sensors. Using multiple sensors can often cause errors in the land

390 use classification due to heterogeneities in the spatial resolution of the data (Joshi et al. 2016;
391 Xie et al. 2008). However, integrating the IKONOS and WV2 data resulted in a smaller error and
392 higher accuracy; this was probably because of the finer resolutions and greater overlap of the
393 wavelength bands. Fine-resolution data may partly resolve such errors by reducing the
394 mismatches in the overlays of wavelength bands.

395 **Conclusion**

396 A DT constructed using a hierarchical classification greatly improved the classification of land
397 use types at a fine resolution. The DT was developed using all of the four examined VIs because
398 each VI demonstrated unique strengths and limitations. For example, the GRVI showed the
399 lowest overall accuracy, but it was retained in the DT because the GRVI can effectively classify
400 areas with a high greenness. The land use classification scheme using the DT clarified that the
401 changes in Purbachal New Town are characterized by the effects of road networks on deeply
402 green ecosystems, which are unlikely to be detected clearly at coarse resolutions. Therefore, this
403 research showed a significant monitoring source to investigate the continuous changes in land
404 use types and assist the planners and decision makers to develop land use management plans.

405 **References**

- 406 Aguilar, M. A., Saldaña, M. M., & Aguilar, F. J. (2013). GeoEye-1 and WorldView-2 pan-
407 sharpened imagery for object-based classification in urban environments. *International*
408 *Journal of Remote Sensing*, 34, 2583–2606.
409 <https://doi.org/10.1080/01431161.2012.747018>.
- 410 Anonymous (2013). *Environmental Impact Assessment (EIA) of Purbachal New Town Project*.
411 Rajdhani Unnayan Kartripakkha (RAJUK), Ministry of Housing and Public Works,
412 Government of the People's Republic of Bangladesh.

- 413 Akay, S. S., & Sertel, E. (2016). Urban land cover/use change detection using high resolution
414 spot 5 and spot 6 images and urban atlas nomenclature. *The International Archives of the*
415 *Photogrammetry, Remote Sensing and Spatial Information Sciences*, XLI-B8, 789–796.
416 XXIII ISPRS Congress, Prague, Czech Republic. [https://doi.org/10.5194/isprs-archives-](https://doi.org/10.5194/isprs-archives-XLI-B8-789-2016)
417 [XLI-B8-789-2016](https://doi.org/10.5194/isprs-archives-XLI-B8-789-2016).
- 418 Barzegar, M., Ebadi, H., & Kiani, A. (2015). Comparison of different vegetation indices for very
419 high-resolution images, specific case UltraCam-D imagery. *Remote Sensing and Spatial*
420 *Information Sciences*, XL-1/W5. <https://doi.org/10.5194/isprsarchives-XL-1-W5-97-2015>.
- 421 Brown De Colstoun, E. C. B., Story, M. H., Thompson, C., Commisso, K., Smith, T. G., & Irons,
422 J. R. (2003). National Park vegetation mapping using multi-temporal Landsat 7 data and
423 a decision tree classifier. *Remote Sensing of Environment*, 85, 316–327.
- 424 Boyle, S. A., Kennedy, C. M., Torres, J., Colman, K., Pérez-Estigarribia, P. E., & de la Sancha,
425 N. U. (2014). High-Resolution Satellite Imagery Is an Important yet Underutilized
426 Resource in Conservation Biology. *PLoS ONE*, 9, e86908.
427 <http://doi.org/10.1371/journal.pone.0086908>.
- 428 Cristiano, P. M., Madanes, N., Campanello, P. I., di Francescantonio, D., Rodríguez, S. A.,
429 Zhang, Y-J., Carrasco, L. O., & Goldstein, G. (2014). High NDVI and potential canopy
430 photosynthesis of south American subtropical forests despite seasonal changes in leaf
431 area index and air temperature. *Forests*, 5, 287–308. doi:[10.3390/f5020287](https://doi.org/10.3390/f5020287).
- 432 Dewan, A. M., & Yamaguchi, Y. (2009). Using remote sensing and GIS to detect and monitor
433 land use and land cover change in Dhaka Metropolitan of Bangladesh during 1960–2005.
434 *Environ Monit Assess*, 150, 237–249. doi: 10.1007/s10661-008-0226-5.
- 435 Dibs, H., Idrees, M. O., & Alsahlin, G. B. A. (2017). Hierarchical classification approach for
436 mapping rubber tree growth using per-pixel and object-oriented classifiers with SPOT-5
437 imagery. *The Egyptian Journal of Remote Sensing and Space Sciences*, 20, 21–30.
438 <http://dx.doi.org/10.1016/j.ejrs.2017.01.004>.
- 439 Erener, A., Düzgün, S., & Yalciner, A. C. (2012). Evaluating land use/cover change with
440 temporal satellite data and information systems. *Procedia Technology*, 1, 385–389.
441 <https://doi.org/10.1016/j.protcy.2012.02.079>.
- 442 Fisher, J. R. B., Acosta, E. A., Dennedy-Frank, P. J., Kroeger, T., & Boucher, T. M. (2017).
443 Impact of satellite imagery spatial resolution on land use classification accuracy and

444 modeled water quality. *Remote Sensing in Ecology and Conservation*, 1-13.
 445 <https://doi.org/10.1002/rse2.61>.

446 Fonji, S. F., & Taff, G. N. (2014). Using satellite data to monitor land-use land-cover change in
 447 North-eastern Latvia. *Springer Plus*, 3(61). <https://doi.org/10.1186/2193-1801-3-61>.

448 Foody, G. M. (2002). Status of land cover classification accuracy assessment. *Remote Sensing of*
 449 *Environment*, 80, 185–201. [https://doi.org/10.1016/S0034-4257\(01\)00295-4](https://doi.org/10.1016/S0034-4257(01)00295-4).

450 Gautam, K. H., & Devoe, N. N. (2006). Ecological and anthropogenic niches of sal (*Shorea*
 451 *robusta* Gaertn. f.) forest and prospects for multiple-product forest management – a
 452 review. *Forestry (Lond)*, 79, 81–101. <https://doi.org/10.1093/forestry/cpi063>.

453 Hasnat, M. M., & Hoque, M. S. (2016). Developing Satellite Towns: A Solution to Housing
 454 Problem or Creation of New Problems. *IACSIT International Journal of Engineering and*
 455 *Technology*, 8, 50–56.

456 Hassan, M. M. (2004). *A study on flora species diversity and their relations with farmers' socio-*
 457 *agro-economic condition in Madhupur Sal forest*. Dissertation, Department of
 458 Agroforestry, Bangladesh Agricultural University, Mymensingh, Bangladesh.

459 Holben, B. N., & Justice, C. O. (1981). An examination of spectral band ratioing to reduce the
 460 topographic effect on remotely sensed data. *International Journal of Remote Sensing*, 2,
 461 115–133. <http://dx.doi.org/10.1080/01431168108948349>.

462 Hossain, S. (2013). Migration, urbanization and poverty in Dhaka, Bangladesh. *Journal of the*
 463 *Asiatic Society of Bangladesh (Hum.)*, 58, 369–382.

464 Huete, A. (1988). A soil-adjusted vegetation index (SAVI). *Remote Sensing of Environment*, 25,
 465 295–309.

466 Huete, A. R., Justice, C., & van Leeuwen, W. (1999). *MODIS Vegetation Index (MOD13)*
 467 *Algorithm Theoretical Basis Document*. Version 3.1. Vegetation Index and Phenology
 468 Lab, The University of Arizona.

469 Huete, A. R., Liu, H. Q., Batchily, K., & van Leeuwen, W. (1997). A Comparison of Vegetation
 470 Indices over a Global set of TM Images for EOS-MODIS. *Remote Sensing of*
 471 *Environment*, 59, 440–451. doi:10.1016/S0034-4257(96)00112-5.

472 Huete, A., Justice, C., & Liu, H. (1994). Development of vegetation and soil indices for MODIS-
 473 EOS. *Remote Sensing of Environment*, 49, 224–234.

474 Huete, A., Didan, K., Miura, T., Rodriguez, E. P., Gao, X., & Ferreira, L. G. (2002). Overview
475 of the Radiometric and Biophysical Performance of the MODIS Vegetation Indices.
476 *Remote Sensing of Environment*, 83, 195–213. doi: [10.1016/S0034-4257\(02\)00096-2](https://doi.org/10.1016/S0034-4257(02)00096-2).

477 Jiang, Z., Huete, A. R., Didan, K., & Miura, T. (2008). Development of a two-band
478 enhanced vegetation index without a blue band. *Remote Sensing of Environment*, 112,
479 3833–3845.

480 Jiang, Z., Huete, A. R., Kim, Y., & Didan, K. (2007). 2-band enhanced vegetation index without
481 a blue band and its application to AVHRR data. *Remote Sensing and Modeling of*
482 *Ecosystems for Sustainability*, 6679 667905, 1–9. <http://dx.doi.org/10.1117/12.734933>.

483 Joshi, Chandra, P. (2011). Performance evaluation of vegetation indices using remotely sensed
484 data. *International journal of geomatics and geosciences*, 2, 231–240. ISSN 0976 – 4380.

485 Joshi, N., Baumann, M., Ehammer, A., Fensholt, R., Grogan, K., Hostert, P., Jepsen, M. R. et al.
486 (2016). A Review of the Application of Optical and Radar Remote Sensing Data Fusion
487 to Land Use Mapping and Monitoring. *Remote Sens*, 8, 70. doi:[10.3390/rs8010070](https://doi.org/10.3390/rs8010070).

488 Julien, Y., Sobrino, J. A., Mattar, C., Ruescas, A. B., Jimé´nez-Munoz, J. C., So`ria, G., Hidalgo,
489 V., Atitar, M., Franch, B., & Cuenca, J. (2011). Temporal analysis of normalized
490 difference vegetation index (NDVI) and land surface temperature (LST) parameters to
491 detect changes in the Iberian land cover between 1981 and 2001. *International Journal of*
492 *Remote Sensing*, 32, 2057–2068. <https://doi.org/10.1080/01431161003762363>.

493 Kalyani, P., & Govindarajulu, P. (2015). Multi-Scale Urban Analysis Using Remote Sensing and
494 GIS. *Geoinformatica: An International Journal (GIJ)*, 5, 1–11.

495 Karnieli, A., Bayarjargal, Y., Bayasgalan, M., Mandakh, B., Dugarjav, C., Burgheimer, J.,
496 Khudulmur, S., Bazha, S. N., & Gunin, P. D. (2013). Do vegetation indices provide a
497 reliable indication of vegetation degradation? A case study in the Mongolian pastures.
498 *International Journal of Remote Sensing*, 34, 6243–6262.
499 <https://doi.org/10.1080/01431161.2013.793865>.

500 Khatun, H., Falgune, N., & Kutub, M. J. R. (2015). Analyzing urban population density
501 gradient of Dhaka Metropolitan Area using Geographic Information Systems (GIS) and
502 Census Data. *Malaysian Journal of Society and Space*, 13, 1–13. ISSN 2180-2491.

503 Kinthada N. R., Gurrarn, M. K., Eadara, A., & Velagala, V. R. (2014). Land Use/Land Cover and
504 NDVI Analysis for Monitoring the Health of Micro-watersheds of Sarada River Basin,
505 Visakhapatnam District, India. *J Geol Geosci*, 3, 146. doi:10.4172/2329-6755.1000146.

506 Kushida, K., Hobara, S., Tsuyuzaki, S., Kim, Y., Watanabe, M., Setiawan, Y., Harada, K.,
507 Shaver, G. R., & Fukuda, M. (2015). Spectral indices for remote sensing of phytomass,
508 deciduous shrubs, and productivity in Alaskan Arctic tundra. *International Journal of*
509 *Remote Sensing*, 36, 4344–4362. <https://doi.org/10.1080/01431161.2015.1080878>.

510 Laliberte, A. S., Fredrickson, E. L., & Rango, A. (2007). Combining decision trees with
511 hierarchical object-oriented image analysis for mapping arid rangelands. *Journal of*
512 *Photogrammetric Engineering and Remote Sensing*, 73, 197–207.

513 Lunetta, R. S., Knight, J. F., Ediriwickrema, J., Lyon, J. G., & Worthy, L. D. (2006). Land-cover
514 change detection using multi-temporal MODIS NDVI data. *Remote Sensing of*
515 *Environment*, 105, 142–154.

516 Mandal, R. A., Yadav, B. K. V., Yadav, K. K., Dutta, I. C., & Haque, S. M. (2013). Biodiversity
517 comparison of natural *Shorea robusta* mixed forest with *Eucalyptus Camaldulensis*
518 plantation in Nepal. *Scholars Academic Journal of Biosciences (SAJB)*, 1, 144–149.

519 Markogianni, V., Dimitriou, E., & Kalivas, D. P. (2013). Land-use and vegetation change
520 detection in Plastira artificial lake catchment (Greece) by using remote sensing and GIS
521 techniques. *International Journal of Remote Sensing*, 34, 1265-1281.
522 <https://doi.org/10.1080/01431161.2012.718454>.

523 Matsushita, B., Yang, W., Chen, J., Onda, Y., & Qiu, G. (2007). Sensitivity of the Enhanced
524 Vegetation Index (EVI) and Normalized Difference Vegetation Index (NDVI) to
525 Topographic Effects: A Case Study in High-Density Cypress Forest. *Sensors*, 7, 2636–
526 2651.

527 Merlotto, A., Piccolo, M. C., & Bertola, G. R. (2012). Urban growth and land use/cover change
528 at Necochea and Quequen cities, Buenos Aires province, Argentina. *Revista de*
529 *Geografia Norte Grande*, 53, 159–176.

530 Miura, T., Huete, A. R., Yoshioka, H., & Holben, B. N. (2001). An error and sensitivity analysis
531 of atmospheric resistant vegetation indices de-rived from dark target-based atmospheric
532 correction. *Remote Sensing of Environment*, 78, 284–298.

533 Motohka, T., Nasahara, K. N., Oguma, H., & Tsuchida, S. (2010). Applicability of green-red
534 Vegetation Index for remote sensing of vegetation phenology. *Remote Sensing*, 2, 2369–
535 2387. doi:[10.3390/rs2102369](https://doi.org/10.3390/rs2102369).

536 Mountrakis, G., Im, J., & Ogole, C. (2011). Support vector machines in remote sensing: a review.
537 *ISPRS J. Photogramm. Remote Sens.*, 66 (3), 247–259.

538 Myneni, R. B., Keeling, C. D., Tucker, C. J., Asrar, G., & Nemani, R. R. (1997). Increased plant
539 growth in the northern high latitudes from 1981 to 1991. *Nature*, 386, 698–702.
540 doi:10.1038/386698a0.

541 Nagai, S., Saitoh, T. M., Kobayashi, H., Ishihara, M., Suzuki, R., Motohka, T., Nasahara, K. N.,
542 & Muraoka, H. (2012). In *situ* examination of the relationship between various
543 Vegetation Indices and canopy phenology in an evergreen coniferous forest, Japan.
544 *International Journal of Remote Sensing*, 33, 6202–6214.

545 Nigam, R. K. (2000). Application of Remote Sensing and Geographical Information System for
546 Land Use / Land Cover Mapping and Change Detection in the Rural Urban Fringe Area
547 of Enschede City, The Netherlands. *International Archives of Photogrammetry and*
548 *Remote Sensing*, 33, 993–998.

549 Nouri, H., Beecham, S., Anderson, S., & Nagler, P. (2014). High Spatial Resolution WorldView-
550 2 Imagery for Mapping NDVI and Its Relationship to Temporal Urban Landscape
551 Evapotranspiration Factors. *Remote Sensing*, 6, 580–602. doi:[10.3390/rs6010580](https://doi.org/10.3390/rs6010580).

552 O'Connell, J., Connolly, J., Vermote, E. F., & Holden, N. M. (2013). Radiometric normalization
553 for change detection in peatlands: a modified temporal invariant cluster approach.
554 *International Journal of Remote Sensing*, 34, 2905–2924.
555 <https://doi.org/10.1080/01431161.2012.752886>.

556 Phompila, C., Lewis, M., Ostendorf, B., & Clarke, K. (2015). MODIS EVI and LST Temporal
557 Response for Discrimination of Tropical Land Covers. *Remote Sensing*, 7, 6026–6040.
558 doi:[10.3390/rs70506026](https://doi.org/10.3390/rs70506026).

559 Pigeon, G., Lemonsu, A., Long, N., Barrié, J., Masson, V., & Durand, P. (2006). Urban
560 thermodynamic island in a coastal city analysed from an optimized surface network.
561 *Boundary-Layer Meteorology*, 120, 315–351.

562 Pijanowski, B. C., Brown, D. G., Shellito, B., & Manik, G. (2002). Using neural networks and
563 GIS to forecast land use changes: a land transformation model. *Computers, Environment
564 and Urban Systems*, 26, 553–575. [https://doi.org/10.1016/S0198-9715\(01\)00015-1](https://doi.org/10.1016/S0198-9715(01)00015-1).

565 Rahman, M. A., Woobaidullah, A. S. M., Quamruzzaman, C., Rahman, M. M., Khan, A. U., &
566 Mustahid, F. (2016a). Probable Liquefaction Map for Purbachal New Town, Dhaka,
567 Bangladesh. *International Journal of Emerging Technology and Advanced Engineering*,
568 6, 345–356.

569 Rahman, M. A., Mostafa Kamal, S. M., & Maruf Billah, M. (2016b). Rainfall Variability and
570 Linear Trend Models on North-West Part of Bangladesh for the Last 40 Years. *American
571 Journal of Applied Mathematics*, 4, 158-162. doi: 10.11648/j.ajam.20160403.16

572 Rocha, A. V., & Shaver, G. R. (2009). Advantages of a two band EVI calculated from solar and
573 photosynthetically active radiation fluxes. *Agricultural and Forest Meteorology*, 149,
574 1560–1563.

575 Rouse, J. W., Haas, R. H., Deering, D. W., Schell, J. A., & Harlan, J. C. (1974). *Monitoring the
576 vernal advancement and retrogradation (green wave effect) of natural vegetation*.
577 Technical Report, No E74-10676, NASA-CR-139243, PR-7. ID: 19740022555. Texas
578 A&M Univ.; Remote Sensing Center. College Station, TX, United States.

579 Sahebjalal, E., & Dashtekian, K. (2013). Analysis of land use-land covers changes using
580 normalized difference vegetation index (NDVI) differencing and classification methods.
581 *African Journal of Agricultural Research*, 8, 4614-4622. doi:10.5897/AJAR11.1825.

582 Salam, M. A., Noguchi, T., & Koike, M. (1999). The causes of forest cover loss in the hill forests
583 in Bangladesh. *GeoJournal*, 47, 539–549.

584 Saleska, S. R., Didan, K., Huete, A. R., da Rocha, H. R. (2007). Amazon forests green-up during
585 2005 drought. *Science*, 318, 612.

586 Sesnie, S. E., Gessler, P. E., Finegan, B., & Thessler, S. (2008). Integrating Landsat TM and
587 SRTM-DEM derived variables with decision trees for habitat classification and change
588 detection in complex neotropical environments. *Remote Sensing of Environment*, 112(5),
589 2145–2159.

590 Shapla, T., Park, J., Hongo, C., & Kuze, H. (2015). Agricultural land cover change in Gazipur,
591 Bangladesh, in relation to local economy studied using Landsat images. *Advances in
592 Remote Sensing*, 4, 214–223. <http://dx.doi.org/10.4236/ars.2015.43017>.

- 593 Singh, R. P., Singh, N., Singh, S., & Mukherjee, S. (2016). Normalized Difference Vegetation
594 Index (NDVI) Based Classification to Assess the Change in Land Use/Land Cover
595 (LULC) in Lower Assam, India. *International Journal of Advanced Remote Sensing and*
596 *GIS*, 5, 1963-1970. doi: <https://doi.org/10.23953/cloud.ijarsg.74>.
- 597 Tucker, C. J. (1979). Red and photographic infrared linear combinations for monitoring
598 vegetation. *Remote Sensing of Environment*, 8, 127–150. [https://doi.org/10.1016/0034-](https://doi.org/10.1016/0034-4257(79)90013-0)
599 [4257\(79\)90013-0](https://doi.org/10.1016/0034-4257(79)90013-0).
- 600 Van Leeuwen, W. J. D., & Huete, A. R. (1996). Effects of standing litter on the biophysical
601 interpretation of plant canopies with spectral indices. *Remote Sensing of Environment*, 55,
602 123–138. [https://doi.org/10.1016/0034-4257\(95\)00198-0](https://doi.org/10.1016/0034-4257(95)00198-0).
- 603 Wardlow, B. D., Egbert, S. L., & Kastens, J. H. (2007). Analysis of time-series MODIS 250 m
604 vegetation index data for crop classification in the U.S. Central Great Plains. *Remote*
605 *Sensing of Environment*, 108, 290–310.
- 606 Xie, Y., Sha, Z., & Yu, M. (2008). Remote sensing imagery in vegetation mapping: a review. *J*
607 *Plant Ecol*, 1, 9–23. <https://doi.org/10.1093/jpe/rtm005>.
- 608 Zaman, A. K. M. A. (2016). *Precarious Periphery: Satellite township development causing*
609 *socio-political economic and environmental threats at the fringe areas of Dhaka*.
610 Unpublished Paper. Department of Architecture, KU Leuven.
611 <https://doi.org/10.13140/rg.2.2.30067.32807>.
- 612 Zar, J. H. (1999). *Biostatistical Analysis*. Department of Biological Sciences, Northern Illinois
613 University. 4th Ed. New Jersey 07458, USA. Prentice Hall, Inc. Simon & Schuster. ISBN
614 0-13-082390-2.
- 615 Zhou, N. Q., & Zhao, S. (2013). Urbanization process and induced environmental geological
616 hazards in China. *Natural Hazards*, 67, 797–810. doi:10.1007/s11069-013-0606-1.